



**HAL**  
open science

## Optimal pose selection for calibration of planar anthropomorphic manipulators

Alexandr Klimchik, Stéphane Caro, Anatol Pashkevich

► **To cite this version:**

Alexandr Klimchik, Stéphane Caro, Anatol Pashkevich. Optimal pose selection for calibration of planar anthropomorphic manipulators. *Precision Engineering*, 2015, 40, pp.214-229. 10.1016/j.precisioneng.2014.12.001 . hal-01204736

**HAL Id: hal-01204736**

**<https://imt-atlantique.hal.science/hal-01204736v1>**

Submitted on 3 May 2018

**HAL** is a multi-disciplinary open access archive for the deposit and dissemination of scientific research documents, whether they are published or not. The documents may come from teaching and research institutions in France or abroad, or from public or private research centers.

L'archive ouverte pluridisciplinaire **HAL**, est destinée au dépôt et à la diffusion de documents scientifiques de niveau recherche, publiés ou non, émanant des établissements d'enseignement et de recherche français ou étrangers, des laboratoires publics ou privés.

# Optimal pose selection for calibration of planar anthropomorphic manipulators

Alexandr Klimchik<sup>a,b,\*</sup>, Stéphane Caro<sup>b,c</sup>, Anatol Pashkevich<sup>a,b</sup>

<sup>a</sup> Ecole des Mines de Nantes, 4 rue Alfred-Kastler, Nantes 44307, France

<sup>b</sup> Institut de Recherche en Communications et Cybernétique de Nantes, UMR CNRS 6597, 1 rue de la Noë, 44321 Nantes, France

<sup>c</sup> Centre National de la Recherche Scientifique (CNRS), Paris, France

The paper is devoted to the calibration experiment design for serial anthropomorphic manipulators with arbitrary number of links. It proposes simple rules for the selection of manipulator configurations that allow the user to essentially improve calibration accuracy and reduce identification errors. Although the main results have been obtained for the planar manipulators, they can be also useful for calibration of more complicated mechanisms. The efficiency of the proposed approach is illustrated with several examples that deal with typical planar manipulators and an anthropomorphic industrial robot.

## 1. Introduction

The standard engineering practice in industrial robotics assumes that the closed-loop control technique is applied only on the level of servo-drives, i.e. for actuating the manipulator joints. In such systems, the Cartesian space control is based on the open-loop method that incorporates numerous direct/inverse kinematic transformations derived from the manipulator geometric model. These transformations define correspondence between the manipulator joint coordinates and the Cartesian coordinates of the end-effector. Hence, to achieve desired accuracy, manipulator geometric model employed in the control algorithm should be carefully tuned (calibrated) to take into account manufacturing tolerances and parameter variations from manipulator to manipulator [1].

The problem of robot calibration has already been well studied and it has been in the focus of research community for many years [2]. In general, the calibration process is divided into four sequential steps [3]: modeling, measurements, identification and compensation. The first step focuses on the design of the appropriate (complete but non-redundant [4]) mathematical model. At the second step, related measurements (calibration experiments) are carried out using commercially available or custom-made

equipments [5,6]. The third step usually deals with the identification of the Denavit–Hartenberg parameters [7], which may provoke numerical instabilities for the manipulators with collinear successive axes considered in this paper. For this particular but very common case, some authors (Hayati [8], Stone [9], and Zhuang [10]) proposed some modifications, but here we will use a more straightforward approach that is more efficient for the planar manipulators. The last step is aimed at compensating identified parameter variations [11–13].

Among numerous publications devoted to the robot calibration, there is a very limited number of works that directly addresses the issue of the identification accuracy and reduction of the calibration errors. In particular, Ikits and Hollerbach [14] used noise amplification index to estimate the errors in the identified parameters of Puma 560 robot. Mirman and Gupta [15] proposed compensation algorithm using position-independent parameter error values. In [16] the authors assessed backlash error for an ABB IRB 1600 6-dof serial industrial robot. Five different observability indexes were compared in [17] and the authors detected that all of them are related to each other. In [18] the determinant-based observability index was used to evaluate the performance of active robot calibration algorithm applied to a 6-dof PUMA 560 robot. In further comparison study, Hollerbach et al. [19] proposed to treat all calibration methods as closed-loop ones and introduced the calibration index that categorizes all calibration methods in terms of number of equations per pose. Zhuang et al. [20] used the condition number of the identification Jacobian to compare the identification accuracy impact of different measurement configurations. In [21] the authors

---

\* Corresponding author at: Ecole des Mines de Nantes, 4 rue Alfred-Kastler, 44307 Nantes, France. Tel.: +33 251 85 83 17; fax: +33 251 85 83 49.

E-mail address: alexandr.klimchik@mines-nantes.fr (A. Klimchik).

used iterative one-by-one pose search algorithm in order to minimize the influence of measurement noise on the identification of geometrical parameters of a Gough-Stewart Platform.

It is clear that the calibration accuracy may be straightforwardly improved by increasing the number of experiments (with the factor  $1/\sqrt{m}$ , where  $m$  is the number of experiments [22]). Besides, using diverse manipulator configurations for different experiments looks also intuitively promising and perfectly corresponds to some basic ideas of the classical theory of experiment design [19] that intends to use experiments that are as much distinct as possible. However, the classical results are mostly obtained for very specific models (such as the linear regression) and cannot be applied here directly due to the non-linearity of the relevant equations. There are few research works in the literature that deal with the optimal pose selection for robot calibration. For example, Borm and Menq [23] have investigated the implications of different observability measures in the robot position error and influence of the measurement configurations number on the final accuracy. They concluded that the number of measurements is less important than proper selection of measurement configurations. In [24] the authors defined the set of optimal measurement configurations by minimizing the condition number of the observation matrix. Daney [25] used the constrained optimization algorithm based on the minimization of the singular values root-product for optimal measurement configurations selection for Gough platform calibration. The noise amplification index was used in [26] to quantify measurement configurations and to select the best one. In [27] authors used D-optimality criteria to determine optimal measurement configurations for planar anthropomorphic manipulators. Zhuang et al. [28] applied simulating annealing to obtain optimal or near optimal measurement configurations, which minimize at least one of two considered performance measures. Imoto et al. [29] proposed to use the end-effector position accuracy after calibration as a performance measure in order to generate measurement configurations. Similar idea was used in [30] where the authors introduced test configurations related to the technological process, which allowed them to define the performance measure as the positioning accuracy after calibration that is also related to the weighted trace of the covariance matrix.

As follows from detailed analysis, all previous works in the area of calibration experiment design provide user with an iterative scheme that aims at minimizing an objective function that depends on the singular values of the identification Jacobian (condition number, for instance). However, this approach does not consider directly the identification accuracy and may lead to some unexpected results (where the condition number is perfect, but the parameter estimation errors are rather high). Besides, it requires very intensive and time consuming computations caused by a poor convergence and high dimension of the search space (number of calibration experiments multiplied by the manipulator joint number). Hence, to apply this technique in industry, strong mathematical background and good experience in the numerical optimization are required. It is obvious that practical engineers need some type of a "rule of thumb", which allows them to select measurement configurations without tedious computations.

In this paper, the problem of optimal design of the calibration experiments is studied for the case of a planar manipulator with arbitrary number of links. Such manipulators do not cover all architectures used in practice, but nevertheless this model allows us to derive some very useful analytical expressions and to propose some simple practical rules defining optimal configurations with respect to the calibration accuracy. In the following sections, particular attention will be given to planar manipulators with 2 and 3 d.o.f. that are essential components of all existing anthropomorphic robots. Practical significance of the obtained results will be illustrated by a case study that deals with the calibration

experiment design for a 6-d.o.f. KUKA industrial robot, which is presented as a set of simple planar sub-manipulators.

The remainder of this paper is organized as follows. Section 2 defines the research problem and contains basic assumptions. Section 3 presents a motivation example that shows the importance of measurement pose selection in robot calibration. In Section 4, the identification algorithm is presented. Section 5 deals with the evaluation of the identification accuracy. Section 6 contains the main theoretical contributions that allow the user to generate desired measurement configurations without straightforward numerical optimization, using proposed rule of thumb. Sections 7 and 8 illustrate advantages of the developed approach and contain some simulation results. In Sections 9 and 10, the proposed technique is extended to the case of spatial manipulator and is applied to a 6-dof serial industrial robot. Section 11 contains discussion where weak and strong sides of the developed approach are considered. Finally, Section 12 summarizes the main contributions of the paper.

## 2. Problem statement

Let us consider a general planar serial manipulator consisting of  $n$  rigid links connected by the corresponding number of revolute joints. For this manipulator, the end-effector position  $(x, y)$  can be defined as follows:

$$\begin{aligned} x &= l_1 \cos q_1 + l_2 \cos (q_1 + q_2) + \dots + l_n \cos (q_1 + q_2 + \dots + q_n) \\ y &= l_1 \sin q_1 + l_2 \sin (q_1 + q_2) + \dots + l_n \sin (q_1 + q_2 + \dots + q_n) \end{aligned} \quad (1)$$

where  $l_1, l_2, \dots, l_n$  are the link lengths,  $q_1, q_2, \dots, q_n$  are the actuated joint coordinates,  $n$  is the number of links. In practice, the actual values of the link length  $l_i$  and the joint coordinates  $q_i$  differ from the nominal ones  $l_i^0$  and  $q_i^0$  by some offsets  $\Delta l_i$  and  $\Delta q_i$  to be identified:

$$l_i = l_i^0 + \Delta l_i; \quad q_i = q_i^0 + \Delta q_i \quad (2)$$

For further convenience, let us introduce the notations

$$\theta_i^0 = \sum_{k=1}^i q_k^0; \quad \Delta \theta_i = \sum_{k=1}^i \Delta q_k \quad (3)$$

that allow us to rewrite (1) as

$$\begin{aligned} x &= (l_1^0 + \Delta l_1) \cdot \cos (\theta_1^0 + \Delta \theta_1) + \dots + (l_n^0 + \Delta l_n) \cdot \cos (\theta_n^0 + \Delta \theta_n) \\ y &= (l_1^0 + \Delta l_1) \cdot \sin (\theta_1^0 + \Delta \theta_1) + \dots + (l_n^0 + \Delta l_n) \cdot \sin (\theta_n^0 + \Delta \theta_n) \end{aligned} \quad (4)$$

Below, the system (4) will be used to generate the set of calibration equations where the offset variables  $\{\Delta l_i, i = \overline{1, n}\}$  and  $\{\Delta \theta_i, i = \overline{1, n}\}$  are treated as unknowns.

To find the desired offsets, a number of experiments are carried out providing a set of Cartesian coordinates  $\{x^k, y^k\}$  and corresponding joint angles  $\{q_1^k, q_2^k, \dots, q_n^k\}$  that theoretically satisfy the system of Eq. (4). However, due to measurement errors, the number of experiments should be excessive and the set of the calibration equations cannot be satisfied simultaneously. Hence, the identification procedure may be treated as the best fitting of the experimental data by the geometrical model (2), i.e. by minimizing the corresponding positional residuals.

To take into account the impact of the measurement noise, the calibration equations derived from (4) can be written in the following form:

$$\begin{aligned} x^k &= \sum_{i=1}^n (l_i^0 + \Delta l_i) \cdot \cos (\theta_i^{0k} + \Delta \theta_i^k) + \varepsilon_x^k \\ y^k &= \sum_{i=1}^n (l_i^0 + \Delta l_i) \cdot \sin (\theta_i^{0k} + \Delta \theta_i^k) + \varepsilon_y^k \end{aligned} \quad (5)$$

where  $k = \overline{1, m}$ , the subscript 'i' defines the manipulator joint/link number, the superscript 'k' indicates the experiment number, the superscript '0' denotes the nominal values of the corresponding variables,  $m$  is the total number of experiments. Besides, it is assumed that the measurement errors  $\{\varepsilon_x^k, \varepsilon_y^k\}$  are independent identically distributed random values (*iid*) with zero mean and the standard deviation  $\sigma$ . It should be noted that, for some technical reasons, the measurement errors in the joint variables  $q_i$  are neglected because of their small impact [31].

In the frame of this model, the desired offsets  $\{\Delta l_i, i = \overline{1, n}\}$  and  $\{\Delta \theta_i, i = \overline{1, n}\}$  computed from the system (5) can be also treated as random variables. Following the main ideas of the statistical estimation theory, it is natural to assume that the mean values of the obtained offsets are equal to their actual values (unbiased estimate) and their standard deviations are as small as possible, i.e.

$$\begin{aligned} E(\widehat{\Delta l_i}) &= \Delta l_i; \quad \text{Var}(\widehat{\Delta l_i}) \rightarrow \min; \quad i = \overline{1, n} \\ E(\widehat{\Delta q_i}) &= \Delta q_i; \quad \text{Var}(\widehat{\Delta q_i}) \rightarrow \min; \quad i = \overline{1, n} \end{aligned} \quad (6)$$

where the hat symbol  $\widehat{\cdot}$  denotes the estimates of the corresponding parameters,  $E(\cdot)$  and  $\text{Var}(\cdot)$  are the expectation and variance, respectively. This generally leads to a multiobjective optimization problem whose solution highly depends on the selection of the manipulator joint coordinates  $\{q_1^k, q_2^k, \dots, q_n^k\}$  used in the calibration experiments. So, the main problem addressed in this paper is to find the set of manipulator configurations (defined by the joint coordinates) that insure the lowest dispersions of  $\widehat{\Delta l_i}$  and  $\widehat{\Delta q_i}$  or certain compromise between them. To make these results attractive for the practicing engineers, the main attention will be paid to the development of simple techniques ("rule of thumb") allowing us to generate the desired configurations without tedious computations, which are required while applying other existing methods (which involve time consuming numerical optimization in multi-dimensional space).

To develop the desired techniques, let us sequentially describe the identification algorithm, evaluate the related identification errors (via the covariance matrix) and develop some optimality conditions (imposed on the joint variables) that guarantee a diagonal structure of the covariance matrix with the smallest elements describing the parameter variances. The latter allows us to reformulate the conventional optimality criteria used in the literature and to present the final solution in a simple geometrical form.

### 3. Motivation example

To demonstrate importance of optimal measurement poses selection in robot calibration, let us present first a simple motivation example. For the purpose of simplicity, let us limit our study to a 2-dof planar manipulator with two *revolute* actuated joints. For this manipulator, the Cartesian coordinates  $x, y$  of the end-effector can be computed as:

$$\begin{aligned} x &= l_1 \cdot \cos q_1 + l_2 \cdot \cos(q_1 + q_2) \\ y &= l_1 \cdot \sin q_1 + l_2 \cdot \sin(q_1 + q_2) \end{aligned} \quad (7)$$

where  $l_1, l_2$  are the link lengths,  $q_1, q_2$  are the actuated joint coordinates. It should be noted that usually real robot parameters  $l_1, l_2$  and  $q_1, q_2$  differ from their nominal values and this manipulator has four geometrical parameters to be identified: (i) two link length deviations  $\Delta l_1, \Delta l_2$ , and (ii) two joint encoder off-sets  $\Delta q_1, \Delta q_2$ .

In order to show the significance of proper measurement configurations selection, let us examine two plans of calibration experiments:

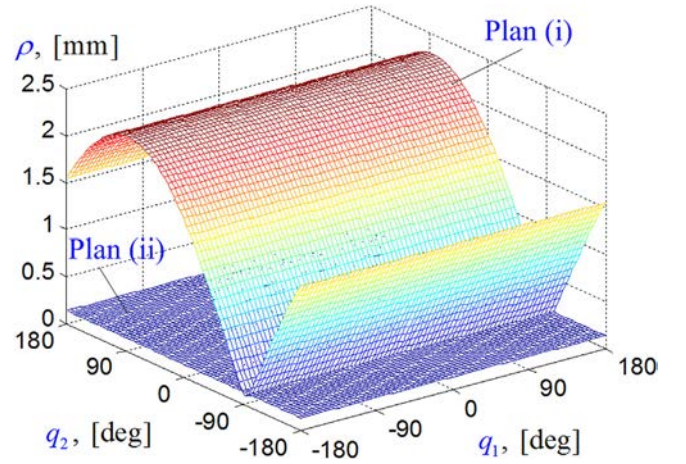


Fig. 1. Positioning accuracy of 2-dof manipulator after calibration using different plans of experiments (measurement noise  $\sigma = 0.1$  mm): plan (i)  $q_1 = 30^\circ, q_2 = -100^\circ$  and  $q_1 = -150^\circ, q_2 = -90^\circ$ ; plan (ii)  $q_1 = 30^\circ, q_2 = -90^\circ$  and  $q_1 = 30^\circ, q_2 = 90^\circ$ .

$$\begin{aligned} \text{Plan (i)} &\{ (q_1 = 30^\circ, q_2 = -100^\circ); (q_1 = -150^\circ, q_2 = -90^\circ) \} \\ \text{Plan (ii)} &\{ (q_1 = 30^\circ, q_2 = -90^\circ); (q_1 = 30^\circ, q_2 = 90^\circ) \} \end{aligned}$$

The first plan has been selected intuitively, while the second one has been generated using results obtained in this work. It should be mentioned that for the considered manipulator each measurement provides two Cartesian coordinates  $x_i, y_i$ . So, the minimum number of measurement configurations is equal to two, it insures the identifiability of all desired parameters  $\Delta l_1, \Delta l_2$  and  $\Delta q_1, \Delta q_2$ .

Using these measurement configurations, simulation of calibration experiments has been done assuming that the measurement noise is Gaussian with zero mean and dispersion  $\sigma = 0.1$  mm. Simulation results for  $l_1 = 0.6$  m,  $l_2 = 0.4$  m are summarized in Fig. 1, where the root-mean-square errors  $\rho$  of the end-effector position after calibration throughout the robot workspace are presented. The figure clearly shows that, in the worst manipulator configuration, the intuitive Plan (i) provides a positioning error equal to 2.29 mm while the proposed Plan (ii) reduces the worst positioning error down to 0.14 mm, i.e. by a factor of 16.

Hence, this simple example clearly shows that selection of measurement configurations is a very important issue in robot calibration. In fact, poorly chosen measurement configurations may have the negative effect and reduce the robot accuracy after calibration. This motivates careful planning of the calibration experiments in order to increase calibration efficiency, which is in the focus of the paper. In the frame of this paper, the calibration efficiency refers to the ability to reduce the impact of measurement errors on the robot accuracy without increasing the number of experiments.

### 4. Identification algorithm

To find the desired parameters using the noise corrupted measurements, the least square technique is usually applied. This approach aims at minimizing the square sum of the residuals in Eq. (5), which is the simplest way to minimize all residuals simultaneously. For the considered problem, the least square objective can be written as:

$$\begin{aligned} &\sum_{k=1}^m \left( \sum_{i=1}^n (l_i^0 + \Delta l_i) \cdot \cos(\theta_i^{0k} + \Delta \theta_i) - x^k \right)^2 \\ &+ \sum_{k=1}^m \left( \sum_{i=1}^n (l_i^0 + \Delta l_i) \cdot \sin(\theta_i^{0k} + \Delta \theta_i) - y^k \right)^2 \rightarrow \min \end{aligned} \quad (8)$$

where  $\{x^k, y^k\}$  and  $\{\theta_1^{0k}, \theta_2^{0k}, \dots, \theta_n^{0k}\}$  denote, respectively, the end-effector Cartesian coordinates and the manipulator joint angles for the  $k$ th experiment,  $l_i^0$  is the nominal length of the  $i$ th link, while  $\Delta l_i$  and  $\Delta \theta_i$  are the offsets to be identified.

Since the unknown variables  $\Delta \theta_i, i = \overline{1, n}$  are incorporated in the trigonometric functions, the optimization problem (8) cannot be solved analytically. On the other hand, in practice the offsets  $\Delta l_i, \Delta \theta_i$  are relatively small. For this reason, the geometrical model (4) can be linearized with respect to the parameters to be identified and presented in a convenient matrix form as

$$\mathbf{P}^k = \mathbf{P}^{0k} + \mathbf{J}^k \cdot \Delta \mathbf{\Pi} \quad (9)$$

where the vector  $\Delta \mathbf{\Pi} = (\Delta \theta_1, \dots, \Delta \theta_n, \Delta l_1, \dots, \Delta l_n)^T$  aggregates all unknown parameters,  $\mathbf{P}^k = (x^k, y^k)^T$  is the end-effector position obtained from the  $k$ th experiment,  $\mathbf{P}^{0k} = (x^{0k}, y^{0k})^T$  is the corresponding end-effector position computed using the nominal values of the link lengths  $l_i^0, i = \overline{1, n}$  and given coordinates  $\{\theta_1^{0k}, \theta_2^{0k}, \dots, \theta_n^{0k}\}$  defining the manipulator configuration for the  $k$ th experiment, i.e.

$$x^{0k} = \sum_{i=1}^n l_i^0 \cos \theta_i^{0k}, \quad y^{0k} = \sum_{i=1}^n l_i^0 \sin \theta_i^{0k}, \quad k = \overline{1, m}, \quad (10)$$

and  $\mathbf{J}^k$  is the calibration Jacobian, which can be computed by differentiating the system (4) with respect to  $\Delta \mathbf{\Pi}$ . After relevant computations the latter can be presented in the form

$$\mathbf{J}^k = \begin{bmatrix} \mathbf{J}_{x\theta}^k & \mathbf{J}_{xl}^k \\ \mathbf{J}_{y\theta}^k & \mathbf{J}_{yl}^k \end{bmatrix}_{2 \times 2n} \quad (11)$$

where

$$\begin{aligned} \mathbf{J}_{x\theta}^k &= - \begin{bmatrix} l_1^0 \sin \theta_1^{0k} & \dots & l_n^0 \sin \theta_n^{0k} \end{bmatrix}_{1 \times n} & \mathbf{J}_{xl}^k &= \begin{bmatrix} \cos \theta_1^{0k} & \dots & \cos \theta_n^{0k} \end{bmatrix}_{1 \times n} \\ \mathbf{J}_{y\theta}^k &= \begin{bmatrix} l_1^0 \cos \theta_1^{0k} & \dots & l_n^0 \cos \theta_n^{0k} \end{bmatrix}_{1 \times n} & \mathbf{J}_{yl}^k &= \begin{bmatrix} \sin \theta_1^{0k} & \dots & \sin \theta_n^{0k} \end{bmatrix}_{1 \times n} \end{aligned} \quad (12)$$

Using the above notation and defining  $\Delta \mathbf{P}^k = \mathbf{P}^k - \mathbf{P}^{0k}$ , the least-square objective (8) can be rewritten as

$$\sum_{k=1}^m (\mathbf{J}^k \cdot \Delta \mathbf{\Pi} - \Delta \mathbf{P}^k)^T (\mathbf{J}^k \cdot \Delta \mathbf{\Pi} - \Delta \mathbf{P}^k) \rightarrow \min \quad (13)$$

which leads to an analytical solution

$$\Delta \mathbf{\Pi} = \left( \sum_{k=1}^m \mathbf{J}^{kT} \mathbf{J}^k \right)^{-1} \cdot \sum_{k=1}^m \mathbf{J}^{kT} \Delta \mathbf{P}^k \quad (14)$$

that will be further used for the accuracy analysis. It should be noted that in the case of relatively large  $\Delta l_i$  and  $\Delta \theta_i$ , the linearization procedure can be applied several times with iterative modifications of the desired geometrical parameters and the configuration variables

$$l_i^0 \leftarrow l_i^0 + \Delta l_i; \quad \theta_i^{0k} \leftarrow \theta_i^{0k} + \Delta \theta_i; \quad \forall i, k \quad (15)$$

This allows us to find a numerical solution of the original optimization problem (8), which cannot be solved analytically.

It should be mentioned that there exist different versions of the above algorithm in the literature, which differ in the type of original measurement data (Cartesian coordinates, distance to the reference point/line, end-effector orientation, etc.) and numerical optimization techniques (gradient search, simulated annealing, genetic algorithms, etc.). Detailed reviews on these issues can be found in [32–40]. In particular, Le et al. [32] grouped sensors to produce 3D data and variety of geometric constraints that allowed them to calibrate all parameters simultaneously. In [33], to increase the accuracy of serial and parallel robots, the authors developed the

Robot Optimization System (ROSY) which uses a dedicated measuring tool with two digital CCD cameras. An alternative geometric parameter identification method that is based on a laser-ranger attached to the end-effector was used in [34]. Kinematic calibration based on differential techniques that uses measurement data from structured laser module and stationary camera was used in [35] to estimate parameters of 7-DOF humanoid manipulator arm. In [36], the authors applied a backpropagation neural network to compensate the joint errors of the neurosurgical robot system. Santolaria et al. [37] utilized the ball bar gauge measurement device and identification technique whose objective function includes terms that are regarding repeatability and measurement accuracy. To improve the static positioning accuracy of the PA10-6CE robot, in [38] a 30-parameter model incorporating elastostatic ones has been used. The screw measurement method that utilizes laser tracker with an active target and identification procedure that is based on circle point analysis was used in [39] to identify the kinematic parameters of an industrial robot. In [40], the authors presented a 12-parameter error kinematic model for the three linear actuators of the Gantry-Tau robot and used three types of measurement equipments (laser interferometers, linear encoders and double-ball bars) to calibrate the linear actuators.

It is also worth mentioning that in practice, there exist non-negligible measurement noise, which is incorporated in the variables  $\Delta \mathbf{P}^k$  indicating the difference between the actual end-effector position (obtained from measurements) and those computed by using the nominal geometrical model. Hence, for the efficient calibration experiment planning, it is reasonable to evaluate the measurement noise impact on the desired manipulator parameters.

## 5. Identification accuracy

To estimate the measurement noise impact on the identification results, let us assume that the manipulator parameters differ from the nominal ones by  $\Delta \hat{\mathbf{\Pi}}$  and the measurements include the additive random errors  $\boldsymbol{\varepsilon}^k = [\varepsilon_x^k, \varepsilon_y^k]^T$  (independent identically distributed with zero mean and standard deviation  $\sigma$ ). This allows us to present the measurement data as

$$\mathbf{P}^k = \mathbf{P}^{0k} + \mathbf{J}^k \cdot \Delta \hat{\mathbf{\Pi}} + \boldsymbol{\varepsilon}^k \quad (16)$$

and, after substitution into (14), to express the identified values as

$$\Delta \mathbf{\Pi} = \Delta \hat{\mathbf{\Pi}} + \left( \sum_{k=1}^m \mathbf{J}^{kT} \mathbf{J}^k \right)^{-1} \cdot \sum_{k=1}^m \mathbf{J}^{kT} \boldsymbol{\varepsilon}^k \quad (17)$$

where the second term is the stochastic component in the model parameter estimation.

As follows from this expression, the considered identification algorithm provides the unbiased estimates

$$E(\Delta \mathbf{\Pi}) = \Delta \hat{\mathbf{\Pi}} \quad (18)$$

where  $E(\cdot)$  denotes the mathematical expectation. Besides, the corresponding covariance matrix defining the identification accuracy, can be expressed as

$$\text{cov}(\Delta \mathbf{\Pi}) = \left( \sum_{k=1}^m \mathbf{J}^{kT} \mathbf{J}^k \right)^{-1} E \left( \sum_{k=1}^m \mathbf{J}^{kT} \boldsymbol{\varepsilon}^k \cdot \sum_{k=1}^m \boldsymbol{\varepsilon}^{kT} \mathbf{J}^k \right) \left( \sum_{k=1}^m \mathbf{J}^{kT} \mathbf{J}^k \right)^{-1} \quad (19)$$

Further, taking into account the statistical properties of the measurement errors (see assumption at the beginning of this section)

$$E(\boldsymbol{\varepsilon}^k \boldsymbol{\varepsilon}^{jT}) = \begin{cases} 0_{2 \times 2}, & k \neq j \\ \sigma^2 \mathbf{I}_{2 \times 2}, & k = j \end{cases} \quad (20)$$

the desired covariance matrix (19) can be presented as

$$\text{cov}(\Delta \mathbf{\Pi}) = \sigma^2 \left( \sum_{k=1}^m \mathbf{J}^{kT} \mathbf{J}^k \right)^{-1} \quad (21)$$

Therefore, the impact of the measurement errors (i.e. the ‘‘quality’’ of the selected measurement configurations  $\{q_1^k, q_2^k, \dots, q_n^k\}$ ) is completely defined by the matrix sum  $\sum_{k=1}^m \mathbf{J}^{kT} \mathbf{J}^k$ , which is constructed from the identification Jacobians.

## 6. Improvement of the identification accuracy via design of calibration experiments

To analyze the above derived matrix (21) in detail, let us take into account that the manipulator model (4) includes two types of identified parameters ( $\Delta l_i$  and  $\Delta \theta_i$ ). So, the sum  $\sum_{k=1}^m \mathbf{J}^{kT} \mathbf{J}^k$  can be presented in the block-wise form as

$$\sum_{k=1}^m \mathbf{J}^{kT} \mathbf{J}^k = \begin{bmatrix} \mathbf{L}^T \mathbf{C} \mathbf{L} & \mathbf{L}^T \mathbf{S} \\ \mathbf{S}^T \mathbf{L} & \mathbf{C} \end{bmatrix} \quad (22)$$

where  $\mathbf{L} = \text{diag}(l_1^0, l_2^0, \dots, l_n^0)$ , while the matrices  $\mathbf{C}$ ,  $\mathbf{S}$  depend on the measurement configurations in the following way:

$$\mathbf{C} = \left[ \sum_{k=1}^m \cos(\theta_i^k - \theta_j^k) \right]_{\substack{i=\overline{1, n} \\ j=\overline{1, n}}} ; \quad \mathbf{S} = \left[ \sum_{k=1}^m \sin(\theta_i^k - \theta_j^k) \right]_{\substack{i=\overline{1, n} \\ j=\overline{1, n}}} \quad (23)$$

where  $\theta_i^k = \sum_{s=1}^i q_s^k$ . It should be mentioned that the diagonal terms of the sub-matrices  $\mathbf{C}$ ,  $\mathbf{S}$  can be computed straightforwardly

$$c_{ii} = m; \quad s_{ii} = 0; \quad \forall i = \overline{1, n}. \quad (24)$$

and do not depend on the measurement configurations. However, the off-diagonal elements highly depend on the selection of the relevant joint angles  $\{q_1^k, q_2^k, \dots, q_n^k\}$ .

It is clear that, using terminology from the classical design of experiments, the sum  $\sum_{k=1}^m \mathbf{J}^{kT} \mathbf{J}^k$  can be treated as the ‘‘information matrix,’’ which may be optimized using several different criteria [22]. The most common ones are so-called *A- and D-optimality criteria*, which allow us to maximize the matrix trace and determinant, respectively. However, the first criterion cannot be applied to the considered problem because the trace of the information matrix (22) does not depend on the design variables  $\{q_1^k, q_2^k, \dots, q_n^k\}$  that define the plan of the calibration experiment. In fact, as follows from expressions (22)–(24), here the trace is constant and is equal to

$$\text{trace} \left( \sum_{k=1}^m \mathbf{J}^{kT} \mathbf{J}^k \right) = m \times n + m \sum_{i=1}^n (l_i^0)^2 \quad (25)$$

Besides, this trace is composed of the elements of different units, which is not acceptable from an engineering view point.

In contrast, the second criterion leads to the optimization problem that produces reasonable and practically acceptable solutions. In this case, using the block-wise formulas of Schur [41], the desired determinant can be expressed as

$$\det \left( \sum_{k=1}^m \mathbf{J}^{kT} \mathbf{J}^k \right) = (\det \mathbf{L})^2 \cdot \det (\mathbf{C} \cdot \mathbf{C}^T - \mathbf{S} \cdot \mathbf{S}^T) \quad (26)$$

where  $\det(\mathbf{L}) = \text{const}$ . As follows from the relevant analysis (see Appendix A), the latter expression reaches its maximum value when all elements of the matrix  $\mathbf{S}$  are equal to zero. This allows us to reformulate the considered problem in the following way

$$\{q_1^k, q_2^k, \dots, q_n^k | k = \overline{1, m}\} = \underset{q}{\text{argmax}} \{ \det \mathbf{C} \} \quad (27)$$

subject to the equality constraint  $S = 0$ . It should be noted that  $\det \mathbf{C} > 0$  here.

Summarizing these results (see Appendix A for details), the optimality conditions of the desired calibration plan can be written as the set of  $n(n-1)$  trigonometric equations

$$\begin{aligned} \sum_{k=1}^m \cos \left( \sum_{s=1}^i q_s^k - \sum_{s=1}^j q_s^k \right) &= 0, \quad \forall i > j \\ \sum_{k=1}^m \sin \left( \sum_{s=1}^i q_s^k - \sum_{s=1}^j q_s^k \right) &= 0, \quad \forall i > j \end{aligned} \quad (28)$$

in  $m \cdot (n-1)$  variables  $\{q_2^k, \dots, q_n^k | k = \overline{1, m}\}$ , where  $i = \overline{1, n}$  and  $j = \overline{i+1, n}$ . It is worth mentioning that the joint variables  $q_1^k$  do not appear in Eq. (28), so the calibrations plans are invariant with respect to the coordinates of the first joint. If those optimality conditions are satisfied, the information matrix will be strictly diagonal since  $\mathbf{S} = 0$  and  $\mathbf{C} = m \mathbf{I}$

$$\sum_{k=1}^m \mathbf{J}^{kT} \mathbf{J}^k = m \begin{bmatrix} \mathbf{L}^2 & \mathbf{0} \\ \mathbf{0} & \mathbf{I} \end{bmatrix} \quad (29)$$

and, as follows from (21), it ensures the minimum values of the variances  $\text{Var}(\Delta l_i)$  and  $\text{Var}(\Delta \theta_i)$ .

Hence, to find the desired set of optimal measurement configurations, it is necessary to solve the underdetermined system of trigonometric Eq. (28), where the number of variables  $m \cdot (n-1)$  is higher than the number of equations  $n(n-1)$ . As a matter of fact,  $m$  is usually greater than  $n$  because the original identification problem (see Section 3) deals with estimation of  $2n$  parameters  $\{\Delta l_i, \Delta \theta_i\}$  using  $2m$  Eq. (4). So, the minimum number of experiments  $m$  ensuring the parameters identifiability is equal to  $n$ . However, in practice  $m > n$ , because it allows reducing the measurement noise impact.

It can be easily proved that the underdetermined system of trigonometric Eq. (28) has an infinite number of solutions. For instance, even in the case of  $n = 2$  and unreasonably small number of measurements  $m = 2$ , the complete set of solutions can be expressed as

$$\begin{aligned} q_1^1 &= \alpha_1; & q_2^1 &= \beta \\ q_1^2 &= \alpha_2; & q_2^2 &= \beta + \pi \end{aligned} \quad (30)$$

where  $\alpha_1, \alpha_2, \beta$  are arbitrary angles within the manipulator joint limits. In more realistic case, when  $n = 2$  and  $m = 3$ , the desired set of solutions

$$\begin{aligned} q_1^1 &= \alpha_1; & q_2^1 &= \beta \\ q_1^2 &= \alpha_2; & q_2^2 &= \beta + \frac{2\pi}{3} \\ q_1^3 &= \alpha_3; & q_2^3 &= \beta - \frac{2\pi}{3} \end{aligned} \quad (31)$$

is defined via four arbitrary angles  $\alpha_1, \alpha_2, \alpha_3, \beta$ . More details concerning the solutions of the considered system for different values of  $m$  and  $n$  are presented in Table 1.

It is worth mentioning that in practice, instead of generating the complete set of solutions of the system (28), it is enough to find an appropriate partial one (since all of them are equivalent with respect to the identification accuracy and provide the same covariance matrix). To find this solution, it is useful to take advantage of the additive structure of the equations defining the optimality conditions for the measurement plans (see Table 1). In fact, these equations can be easily separated into several independent groups

**Table 1**  
Optimality conditions for measurement pose selection: calibration of typical planar manipulators.

Manipulator	Equations defining optimal measurement poses
2-Links manipulator	$\sum_{k=1}^m \cos q_2^k = 0; \sum_{k=1}^m \sin q_2^k = 0,$
3-Links manipulator	$\sum_{k=1}^m \cos q_2^k = 0; \sum_{k=1}^m \sin q_2^k = 0; \sum_{k=1}^m \cos q_3^k = 0; \sum_{k=1}^m \sin q_3^k = 0;$
4-Links manipulator	$\sum_{k=1}^m \cos q_2^k = 0; \sum_{k=1}^m \sin q_2^k = 0; \sum_{k=1}^m \cos q_3^k = 0; \sum_{k=1}^m \sin q_3^k = 0; \sum_{k=1}^m \cos q_4^k = 0; \sum_{k=1}^m \sin q_4^k = 0;$

comprising non-identical variables. For instance, in the simplest case  $n = 2$ , the optimality conditions

$$\sum_{k=1}^m \cos q_2^k = 0; \sum_{k=1}^m \sin q_2^k = 0 \quad (32)$$

can be rewritten as

$$\begin{aligned} \sum_{k=1}^{m_1} \cos q_2^k + \sum_{k=m_1+1}^m \cos q_2^k &= 0 \\ \sum_{k=1}^{m_1} \sin q_2^k + \sum_{k=m_1+1}^m \sin q_2^k &= 0 \end{aligned} \quad (33)$$

and replaced by stronger conditions

$$\begin{aligned} \sum_{k=1}^{m_1} \cos q_2^k = 0; \sum_{k=m_1+1}^m \cos q_2^k &= 0 \\ \sum_{k=1}^{m_1} \sin q_2^k = 0; \sum_{k=m_1+1}^m \sin q_2^k &= 0 \end{aligned} \quad (34)$$

which is obviously sufficient but not necessary with respect to (32). Nevertheless, the desired information matrix (29) is achieved and the identification accuracy does not suffer from this intuitive simplification. It is clear that similar approach can be also applied in general case (for  $n \geq 2$ ).

The above presented idea allows us to propose a heuristic approach for obtaining partial solutions of (28) for any given  $m$  using general solutions for the problems of lower dimensions. Below, this techniques will be referred to as the “superposition of low-dimensional plans”. In practice, the most attractive and sufficient (for our problem) is the decomposition of the sums (28) into several sub-sums of size  $m_1 = 2$  and  $m_2 = 3$ , which is equivalent to the presentation of experiment number  $m$  in the following form

$$m = 2k_1 + 3k_2 \quad (35)$$

where  $k_1, k_2$  are some integers. It is obvious that the partitioning (35) is not unique (and exists if  $m \geq 2$ ), but any of possible presentations is suitable here. For example, for  $n = 2$  the desired solution can be easily composed of  $k_1$  measurement configurations of the type (30) and  $k_2$  configurations of the type (31). Besides, in some cases it is possible to compose optimal plans using one type of configurations only: either type (30) (i.e.  $k_2 = 0$  and  $k_1 = m/2$ ) or type (31) (i.e.  $k_1 = 0$  and  $k_2 = m/3$ ). In the case when  $m$  is a multiple of 6, both mentioned plans of experiments can be used. For instance, for  $m = 6$  the plans  $2 \times 3$  and  $3 \times 2$  are acceptable.

To evaluate visually the diversity of the obtained measurement configurations, Table 2 contains several case studies corresponding to 2-, 3- and 4-link manipulators. As follows from them, the optimal configurations differ essentially from each other, in order to ensure both parameters identifiability and low identification errors. This perfectly suits the basic ideas of the design of experiment theory.

In general, the proposed approach can be treated as a simple rule of thumb allowing to generate easily optimal poses for calibration of planar anthropomorphic manipulators. Applying this rule, it is possible to obtain the measurement configurations that provide the following covariance matrix for the parameters of interest  $\{\Delta l_i, \Delta \theta_i | i = \overline{1, n}\}$  (as well as for the parameters  $\{\Delta l_i, \Delta q_i | i = \overline{1, n}\}$ )

$$\text{cov}(\Delta \Pi) = \frac{\sigma^2}{m} \cdot \begin{bmatrix} \mathbf{L}^{-2} & \mathbf{0} \\ \mathbf{0} & \mathbf{I} \end{bmatrix} \quad (36)$$



**Table 2**  
Optimal measurement configurations for typical planar manipulators.

Manipulator	Number of measurement configurations	Configurations			
		Configuration #1	Configuration #2	Configuration #3	Configuration #4
2-link manipulator $n = 2$	$m = 2$	(0°, 90°) 	(0°, -90°) 		
	$m = 3$	(0°, 0°) 	(0°, 120°) 	(0°, -120°) 	
3-link manipulator $n = 3$	$m = 3$	(0°, 0°, 0°) 	(0°, 120°, 120°) 	(0°, -120°, -120°) 	
	$m = 4$	(0°, -60°, 60°) 	(0°, -120°, -60°) 	(0°, 120°, -120°) 	(0°, 60°, 120°) 
4-link manipulator $n = 4$	$m = 4$	(0°, -60°, 60°, -60°) 	(0°, -120°, -60°, -120°) 	(0°, 120°, -120°, 120°) 	(0°, 60°, 120°, 60°) 

which allows to estimate the identification accuracy via the variances

$$\text{Var}(\Delta q_i) = \frac{\sigma^2}{m \cdot l_i^2}; \quad \text{Var}(\Delta l_i) = \frac{\sigma^2}{m} \quad (37)$$

where  $\sigma$  is the s.t.d. of the measurement noise and  $i = \overline{1, n}$ . These results show that, if the optimal calibration plan is used, the identification errors for the linear parameters  $\Delta l_i$  will depend on the number of experiments only, while the errors for the angular parameter  $\Delta q_i$  will also depend on the link lengths. In more details, the results related to the identification accuracy are presented in Table 3.

Hence, using the proposed rule of thumb one can easily generate the desired measurement configurations corresponding to the D-optimality criteria, which yields essential reduction of the identification errors. It is proved that, from the algebraic point of view, these configurations satisfy the optimality conditions, which require relevant sums of  $\sin(\cdot)$  and  $\cos(\cdot)$  of the joint coordinates to be equal to zero. Using geometrical approach, this rule can be represented on the unit circle, where the sum of corresponding unit vectors must be zero. The latter allows user to find the desired configurations easily. The advantages of this approach are illustrated in the following Sections.

## 7. Simulation study

To demonstrate the efficiency of the proposed technique, let us present some simulation results that deal with two-, three- and

four-links manipulators and employ different calibration plans. The first plan (a conventional one) is based on the regular grid in the joint coordinate space. The second calibration plan implements the proposed strategy, which is described in detail in Section 6. The simulation study has been carried out for different number of experiments ( $m=4 \dots 20$ ); it was assumed that the s.t.d. of the measurement errors is equal to  $\sigma = 0.1$  mm. To obtain reliable results, the simulations have been repeated 10,000 times and averaged.

The manipulator parameters used for the simulations are presented in Table 4. It was assumed that the link lengths are in the range of 100...260 mm, while the geometric errors in the link lengths may be from 0.4 to 1.5 mm and the joint off-sets are 0.3...0.7°. This table also contains the summary of the simulation results for 4 and 20 calibration experiments, which are in good agreement with expressions (37).

To show benefits of the proposed calibration plans, Fig. 1 contains more detailed results corresponding to the conventional and proposed approaches (for the case of 4-links planar manipulator). As follows from them, the optimal pose selection for the calibration experiments allows us to reduce the identification errors by a factor of 1.5–2. For instance, for the number of calibration experiments  $m = 10$  the proposed technique allows us to obtain the s.t.d. of the identification accuracy 0.032 mm for the parameters  $L_1, \dots, L_4$  and from 0.007° to 0.016° for the parameters  $q_1, \dots, q_4$ . In contrast, for the conventional technique, corresponding values are 0.045...0.060 mm and 0.010°...0.027°, respectively. Thus, a simple and practically convenient “rule of thumb” developed in this paper



**Table 3**  
Identification accuracy for manipulator geometric parameters.

Manipulator	$\sum_{k=1}^m \mathbf{J}^k \mathbf{J}^k$	Identification accuracy
2-Links manipulator	$\text{diag}(m \cdot l_1^2, m \cdot l_2^2, m, m)$	$\sigma_{q_1} = \frac{\sigma}{\sqrt{m} \times l_1}$ ; $\sigma_{q_2} = \frac{\sigma}{\sqrt{m} \times l_2}$ ; $\sigma_{L_1} = \frac{\sigma}{\sqrt{m}}$ ; $\sigma_{L_2} = \frac{\sigma}{\sqrt{m}}$
3-Links manipulator	$\text{diag}(m \cdot l_1^2, m \cdot l_2^2, m \cdot l_3^2, m, m, m)$	$\sigma_{q_1} = \frac{\sigma}{\sqrt{m} \times l_1}$ ; $\sigma_{q_2} = \frac{\sigma}{\sqrt{m} \times l_2}$ ; $\sigma_{q_3} = \frac{\sigma}{\sqrt{m} \times l_3}$ ; $\sigma_{L_1} = \frac{\sigma}{\sqrt{m}}$ ; $\sigma_{L_2} = \frac{\sigma}{\sqrt{m}}$ ; $\sigma_{L_3} = \frac{\sigma}{\sqrt{m}}$
4-Links manipulator	$\text{diag}(m \cdot l_1^2, m \cdot l_2^2, m \cdot l_3^2, m \cdot l_4^2, m, m, m, m)$	$\sigma_{q_1} = \frac{\sigma}{\sqrt{m} \times l_1}$ ; $\sigma_{q_2} = \frac{\sigma}{\sqrt{m} \times l_2}$ ; $\sigma_{q_3} = \frac{\sigma}{\sqrt{m} \times l_3}$ ; $\sigma_{q_4} = \frac{\sigma}{\sqrt{m} \times l_4}$ ; $\sigma_{L_1} = \frac{\sigma}{\sqrt{m}}$ ; $\sigma_{L_2} = \frac{\sigma}{\sqrt{m}}$ ; $\sigma_{L_3} = \frac{\sigma}{\sqrt{m}}$ ; $\sigma_{L_4} = \frac{\sigma}{\sqrt{m}}$

**Table 4**  
Identification accuracy for manipulator geometric parameters: simulation study ( $\sigma = 0.1$  mm).

Manipulator	Model parameters	Identification accuracy for optimal plans	
		4 Calibration experiments	20 Calibration experiments
2-Links manipulator	$L_1 = 260$ mm, $\Delta L_1 = 1.5$ mm, $\Delta q_1 = 0.5^\circ$	$\sigma_{L_1} = 0.050$ mm, $\sigma_{q_1} = 0.011^\circ$	$\sigma_{L_1} = 0.022$ mm, $\sigma_{q_1} = 0.005^\circ$
	$L_2 = 180$ mm, $\Delta L_2 = -0.6$ mm, $\Delta q_2 = -0.5^\circ$	$\sigma_{L_2} = 0.050$ mm, $\sigma_{q_2} = 0.016^\circ$	$\sigma_{L_2} = 0.022$ mm, $\sigma_{q_2} = 0.007^\circ$
3-Links manipulator	$L_1 = 260$ mm, $\Delta L_1 = 1.5$ mm, $\Delta q_1 = 0.5^\circ$	$\sigma_{L_1} = 0.050$ mm, $\sigma_{q_1} = 0.011^\circ$	$\sigma_{L_1} = 0.022$ mm, $\sigma_{q_1} = 0.005^\circ$
	$L_2 = 180$ mm, $\Delta L_2 = -0.6$ mm, $\Delta q_2 = -0.5^\circ$	$\sigma_{L_2} = 0.050$ mm, $\sigma_{q_2} = 0.016^\circ$	$\sigma_{L_2} = 0.022$ mm, $\sigma_{q_2} = 0.007^\circ$
	$L_3 = 120$ mm, $\Delta L_3 = -0.4$ mm, $\Delta q_3 = 0.7^\circ$	$\sigma_{L_3} = 0.050$ mm, $\sigma_{q_3} = 0.024^\circ$	$\sigma_{L_3} = 0.022$ mm, $\sigma_{q_3} = 0.011^\circ$
4-Links manipulator	$L_1 = 260$ mm, $\Delta L_1 = 1.5$ mm, $\Delta q_1 = 0.5^\circ$	$\sigma_{L_1} = 0.050$ mm, $\sigma_{q_1} = 0.011^\circ$	$\sigma_{L_1} = 0.022$ mm, $\sigma_{q_1} = 0.005^\circ$
	$L_2 = 180$ mm, $\Delta L_2 = -0.6$ mm, $\Delta q_2 = -0.5^\circ$	$\sigma_{L_2} = 0.050$ mm, $\sigma_{q_2} = 0.016^\circ$	$\sigma_{L_2} = 0.022$ mm, $\sigma_{q_2} = 0.007^\circ$
	$L_3 = 120$ mm, $\Delta L_3 = -0.4$ mm, $\Delta q_3 = 0.7^\circ$	$\sigma_{L_3} = 0.050$ mm, $\sigma_{q_3} = 0.024^\circ$	$\sigma_{L_3} = 0.022$ mm, $\sigma_{q_3} = 0.011^\circ$
	$L_4 = 100$ mm, $\Delta L_4 = 0.7$ mm, $\Delta q_4 = -0.3^\circ$	$\sigma_{L_4} = 0.050$ mm, $\sigma_{q_4} = 0.029^\circ$	$\sigma_{L_4} = 0.022$ mm, $\sigma_{q_4} = 0.013^\circ$

has obvious advantages and is very attractive from an engineering and practical view point.

## 8. Comparison analysis

To illustrate the advantages of the developed technique, let us consider an example of 3-link manipulator whose variations in joint coordinates are limited to the range of  $\pm 100^\circ$ . These limitations are quite common for industrial robots. The considered manipulator includes three linear and three angular geometrical parameters that should be identified by means of calibration. For comparison purposes three different plans of experiments are considered:

- (i) regular plan within the joint limits;
- (ii) random plan within the joint limits; and
- (iii) plan of experiments that satisfies optimality conditions (28) and takes into account the joint limits.

It should be noted that the approach for optimal measurement configurations selection proposed in [23], which also insures conditions (28), is not applicable here, since joint limits do not allow us to generate regular plan of experiments within the whole joint space, i.e.  $\pm 180^\circ$  for each variable (Fig. 2).

For all plans of experiments, the same number of measurements  $m = 64$  has been used (this value has been chosen to have four different angles  $q_1$ ,  $q_2$  and  $q_3$  for the case of regular plan). In the plans (i) and (ii), all measurement configurations are different, while in plan (iii) the measurements have been repeated 16 times for 4 optimal configurations. The link lengths have been assigned to 1.25 m, 1.10 m and 0.23 m (those values corresponds to the link lengths of Kuka industrial robot used in experimental study), the measurements noise parameter was  $\sigma = 0.1$  mm. The identification accuracy of three examined plans of experiments is presented in Table 5. The results show that the proposed plan of calibration experiments allows us to increase essentially the parameters identification accuracy with respect to the random and regular plans (from 20% to 60%). Corresponding improvement of the robot positioning accuracy is presented in Fig. 3, which contains three plots showing scattering of the end-effector location after calibration due to random nature of the measurement errors in the following

**Table 5**  
Comparison of parameters identification accuracy for different calibration plans.

Parameters	Identification accuracy		
	Random plan	Regular plan	Optimal plan
$\Delta \theta_1$ (mrad)	0.012	0.012	0.010
$\Delta \theta_2$ (mrad)	0.017	0.016	0.011
$\Delta \theta_3$ (mrad)	0.075	0.067	0.054
$\Delta L_1$ (mm)	0.015	0.015	0.013
$\Delta L_2$ (mm)	0.019	0.018	0.013
$\Delta L_3$ (mm)	0.017	0.015	0.013

configuration  $q_1 = 0^\circ$ ,  $q_2 = -90^\circ$  and  $q_3 = 90^\circ$ . The value  $\rho$  in Fig. 3 denotes the dispersion of the end-effector errors computed using particular randomly generated data.

An additional study has been performed for the density of points in the regular plan. The same calibration experiments has been performed with 2, 4, 8, 16 and 25 regular spaced points per joint. For each case, the improvement factor has been computed, which shows the benefits of increasing the number of measurement configurations on the parameters identification accuracy. For comparison purposes, the expected improvement factors have been also computed, which corresponds to repeating experiments in the same configurations several times. Simulation results are summarized in Table 6, they show that increasing the number of configurations up to 16,256 does not allow us to increase the identification accuracy more than by 2% comparing with the repeating experiments in 64 reference configurations. This confirms that points density augmentation in the regular plan does not leads to appreciable efficiency improvement, the main accuracy improvement is achieved here due to increasing the number of measurements.

Hence, this example shows that by using limited number of optimal measurement configurations and repeating experiments several times, it is possible to achieve better accuracy than using huge number of configurations distributed within the joint limits. So, the proposed approach speeds up the calibration process without losing the identification accuracy, i.e. improves its efficiency.

Let us also show the benefits of the proposed approach for the measurement configuration selection compared to the techniques based on the conventional observability indices [17]. It was shown

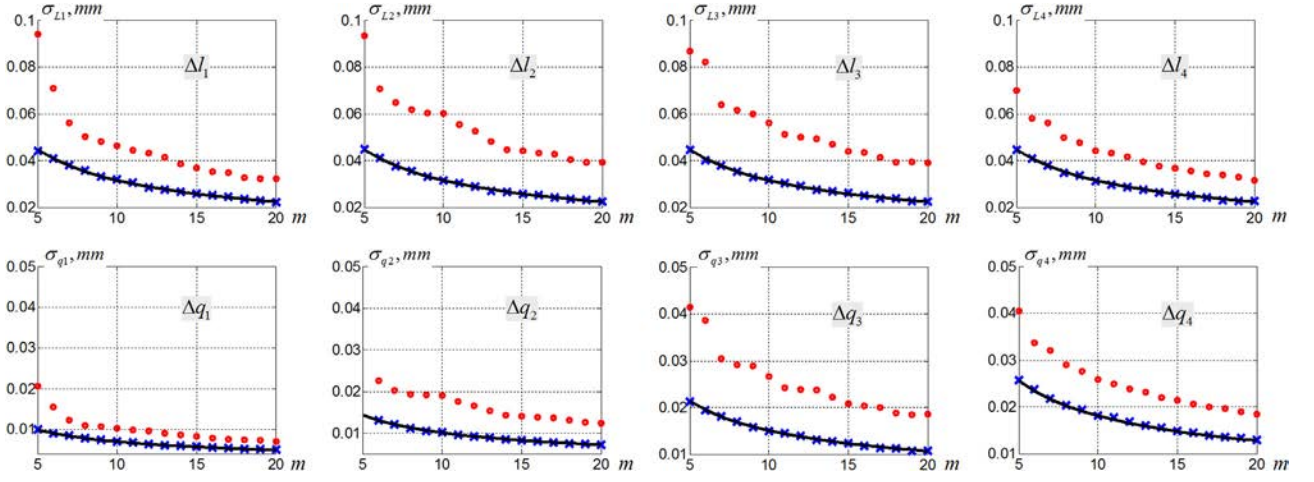


**Fig. 2.** Comparison of the identification accuracy for different calibrations plans (case of 4-links planar manipulator): -- are analytical curves corresponding to the proposed optimal plan (expressions (36)); "x" are experimental results corresponding to the optimal calibration plan (simulation); "o" are experimental results corresponding to the calibration plan with regular grid (simulation).

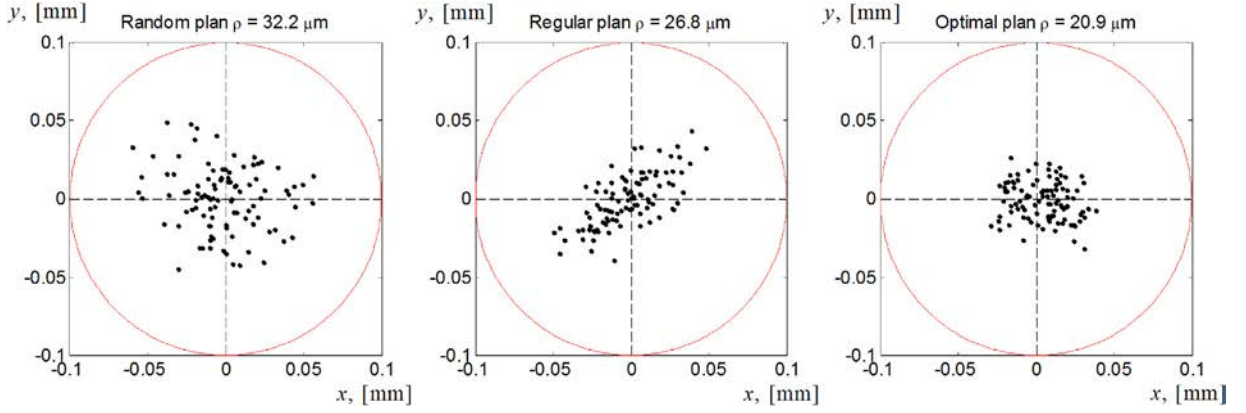


**Fig. 3.** Geometrical error compensation efficiency for different calibration plans of experiments (3-dof planar manipulator, identification of six geometrical parameters, 64 measurement configurations, measurement noise parameter  $\sigma = 0.1$  mm, manipulator configuration  $q_1 = 0^\circ$ ,  $q_2 = -90^\circ$ ,  $q_3 = 90^\circ$ ).

before [42] that all these indices give similar results in terms of identification accuracy. Here, the comparison analysis is done using the same example of the 3-link planar manipulator with the joint limits  $\pm 100^\circ$ . For each performance measures  $O_1-O_5$ , four measurement configurations have been found, which are optimal in terms of the corresponding observability index. It should be mentioned that to generate optimal configurations using conventional techniques, each case requires solution of non-trivial optimization problem with 12 variables (4 measurement configurations). The obtained optimal configurations are presented schematically

in Fig. 4. As follows from it, the obtained solutions are distributed in the robot workspace and differ from one case to another. It should be mentioned that all sets of measurement configurations ensure the same parameters identification accuracy that is equal to the accuracy of the developed technique (see optimal plan in Table 5). Moreover, the values of the observability indices are equal for all obtained plans of experiments (Table 7). Another important conclusion is that for the considered manipulator the positioning accuracy after calibration (using optimal measurement configurations) does not vary essentially within the robot workspace (see Table 7), the

**Table 6**  
Improvement of parameter identification accuracy due to increasing the measurement configuration density for regular plan.

	Number of regular spaced points per joint				
	2	4	8	16	25
Total number of configurations	8	64	512	4096	15,625
Parameters	Improvement factors				
$\Delta\theta_1$	0.33	1	2.86	8.12	15.9
$\Delta\theta_2$	0.32	1	2.88	8.18	16.0
$\Delta\theta_3$	0.33	1	2.86	8.12	15.9
$\Delta L_1$	0.33	1	2.86	8.12	15.9
$\Delta L_2$	0.32	1	2.88	8.18	16.0
$\Delta L_3$	0.33	1	2.86	8.12	15.9
Expected	0.35	1	2.83	8.00	15.6

\* This case have been chosen as a reference one.

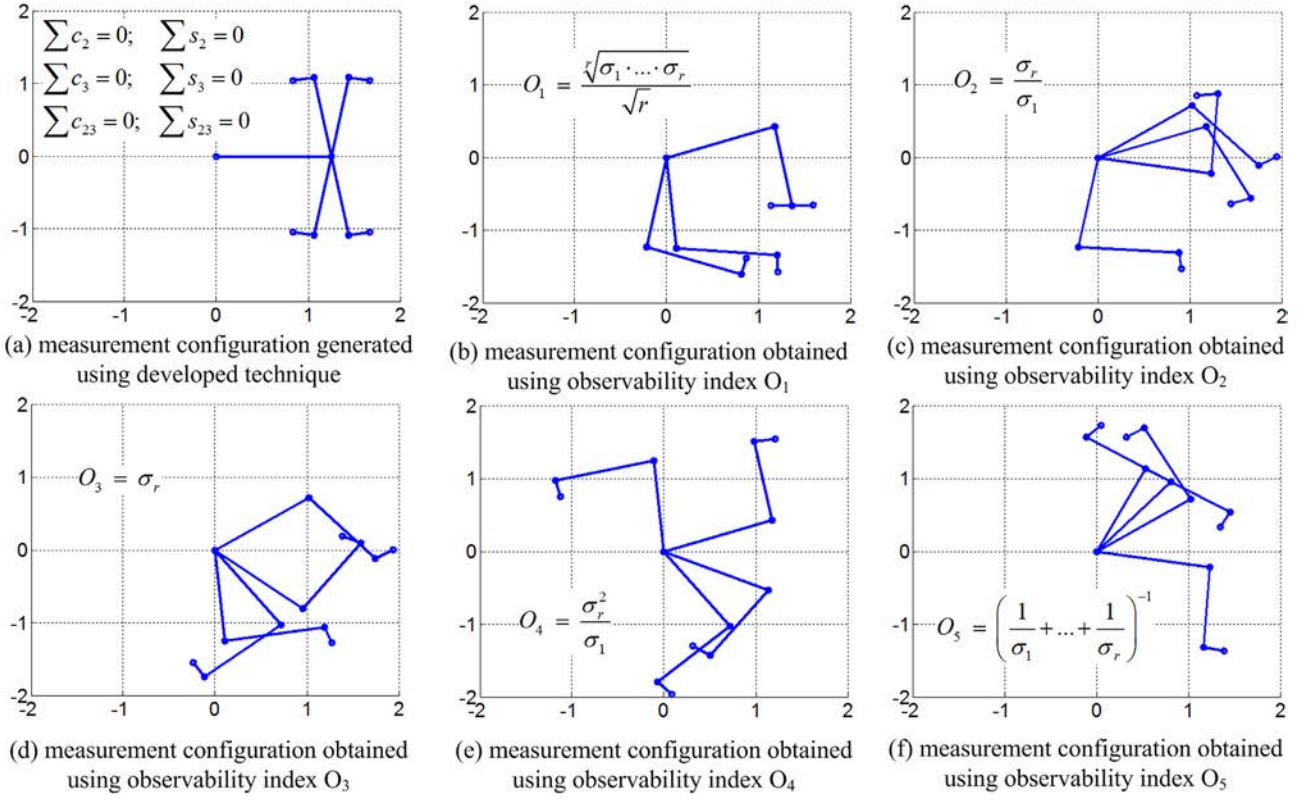


**Fig. 4.** Schematic presentation of optimal measurement configurations for 3-link planar manipulator obtained using the developed technique and conventional observability indices.

difference between maximal and root mean square errors is lower than 0.1%. Hence, the developed technique gives also good results comparing with the test-pose approach proposed in [43], but its obvious advantage is extra-simplicity (it does not require application any numerical optimization routine).

To make graphical presentation more clear, it is useful to take into account that the angle  $q_1$  does not effect on the identification accuracy. So, in optimal plan of experiments,  $q_1$  can be fixed to any arbitrary value. Hence, in order to make comparison analysis easier, it is reasonable to fix the angle  $q_1$  to the same constant value in all obtained plans of experiments ( $q_1 = 0$ , for instance). After such modifications, the obtained optimal configurations become semi-symmetrical (Fig. 5). Besides, in all cases ( $O_1 - O_5$ ) the measurement configurations satisfy the proposed optimality conditions (28), i.e. all plans of experiments are optimal in terms of the developed rule. However, in contrast to the cases  $O_1 - O_5$ , the developed technique allows us to generate optimal measurement configurations without solving optimization problem. This advantage becomes extremely

important with increasing of the number of actuated joints and the number of measurement configurations. In particular, for a 6-dof manipulator and 20 measurement configurations, conventional techniques require solution of an optimization problem with 120 unknowns. This high-dimensional problem is very time consuming and no one can guaranty that the obtained solution the global optimum. In contrast, the developed technique allows user to get the optimum without solving the optimization problem.

## 9. Extension to the 3D case

In spite of numerous advantages, the proposed approach has essential limitations. They are related to the manipulator architecture, for which the optimality conditions are formulated and strictly proved. In fact, the manipulator topology described by Eq. (2) includes 2D serial planar mechanisms with *revolute* joints only. Although generalization for the case of *prismatic* joints is trivial,

**Table 7**  
Performances measures for measurement configurations generated using different optimality criteria.

Performance measures	$O_1 : \frac{\sqrt{\sigma_1 \dots \sigma_r}}{\sqrt{r}} \rightarrow \max$	$O_2 : \frac{\sigma_r}{\sigma_1} \rightarrow \max$	$O_3 : \sigma_r \rightarrow \max$	$O_4 : \frac{\sigma_r^2}{\sigma_1} \rightarrow \max$	$O_5 : \left( \frac{1}{\sigma_1} + \dots + \frac{1}{\sigma_r} \right)^{-1} \rightarrow \max$	Developed technique
$O_1$	0.67	0.67	0.67	0.67	0.67	0.67
$O_2$	0.18	0.18	0.18	0.18	0.18	0.18
$O_3$	0.46	0.46	0.46	0.46	0.46	0.46
$O_4$	0.08	0.08	0.08	0.08	0.08	0.08
$O_5$	0.22	0.22	0.22	0.22	0.22	0.22
Positioning error (max/ $\sigma$ )	1.22	1.22	1.22	1.22	1.22	1.22
Positioning error (RMS/ $\sigma$ )	1.22	1.22	1.22	1.22	1.22	1.22

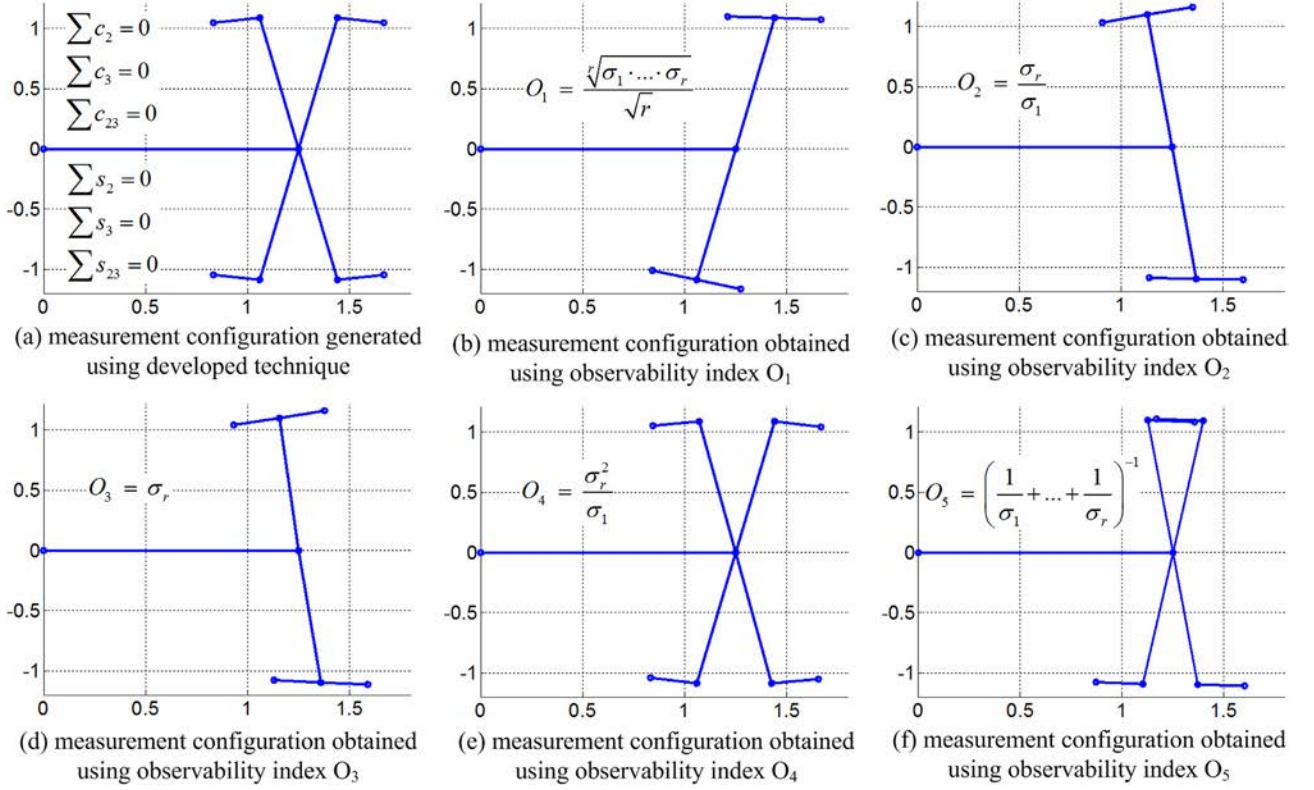


**Fig. 5.** Schematic presentation of modified optimal measurement configurations for a 3-link planar manipulator obtained using the developed technique and conventional observability indices (with  $q_1 = 0$ ).

extension to the 3D case is non obvious and requires additional efforts.

The simplest way to extend the proposed “rule of thumb” to the 3D case is to apply the following procedure:

*Step (a):* decompose the spatial manipulator into a set of planar serial sub-chains;

*Step (b):* apply the developed rule to each sub-chain separately, without assigning certain values to the joint coordinates that can be selected arbitrary;

*Step (c):* aggregate the obtained sub-chain joint coordinates in order to find configurations of the entire manipulator (where some values are still arbitrary);

*Step (d):* apply the developed rule to the each set of the arbitrary coordinates, i.e. ensuring that the sums of sines and cosines are equal to zero for all of them.

To show the efficiency of this heuristic extension, let us consider several typical manipulator architectures used in industry:

(i) *3-Axis SCARA robot* with 2 *revolute* and one *prismatic* joints ( $R_z R_z P_z$  architecture). For this architecture, the rule of thumb can be applied straightforwardly since motions in the  $xy$ -plane and in  $z$ -direction are not coupled. This manipulator can be easily decomposed in two sub-chains corresponding to 2-link planar  $R_z R_z$  manipulator and 1-axis *prismatic*  $P_z$  mechanism. For the first one, the optimal solution is provided by Eq. (28). For the second one, the optimal solution is trivial and is defined by the classical design of experiment theory [22].

(ii) *4-Axis SCARA robot* with 3 *revolute* and one *prismatic* joints ( $R_z R_z P_z R_z$  architecture). Taking into account that this architecture is nominally equivalent to  $R_z R_z R_z P_z$  one, here decomposition leads to  $R_z R_z R_z$  and  $P_z$  mechanisms. So, the

optimal solutions are obtained in similar way: using results for 3-link planar manipulator and 1-axis *prismatic* mechanism.

(iii) *2-Axis articulated robot* with two *revolute* joints ( $R_z R_y$  architecture). In this case, decomposition yields two trivial sub-chains of  $R_z$  and  $R_y$  types. As follows from (28), at the beginning of each separate sub-chain, the joint coordinates can be set arbitrary. However, applying *Step (d)* of the above presented procedure to the joint  $R_y$ , one can get values of the corresponding joint coordinates ensuring zero sums of the sines and cosines. It can be easily verified that the latter operation yields a diagonal information matrix (without applying *Step (d)* to the first joint  $R_z$ ).

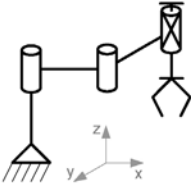
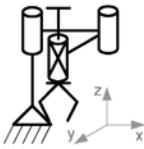
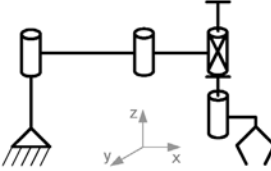
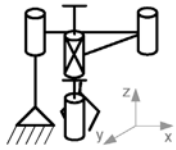
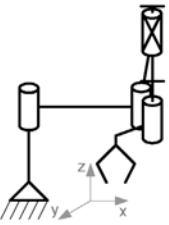
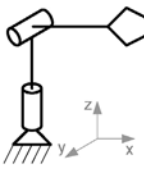
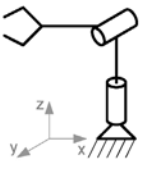
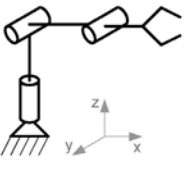
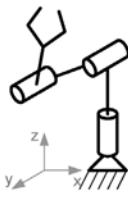

(iv) *3-Axis articulated robot* with three *revolute* joints ( $R_z R_y R_y$  architecture). Here, decomposition leads to a trivial sub-chain  $R_z$  and a 2-link planar manipulator  $R_y R_y$ . They are treated in the same way as the above presented  $R_z R_y$  case, allowing the first joint  $R_z$  to be set arbitrary. Similarly, obtained measurement configurations ensure diagonal structure of the information matrix.

Optimal measurement configurations for the above considers spatial manipulators are presented in Table 8, which also contains corresponding information matrices that are strictly diagonal. They give certain compromise between the identification accuracy of different manipulator parameters that is acceptable from a practical point of view, but obviously is not unique.

Hence, extension of the rule of thumb to the 3D case is rather simple, while it has been derived intuitively, using some heuristic ideas. Nevertheless, dedicated studies confirm that the results are quite good but perhaps not optimal with respect to some parameters. Therefore, the general (and strict) solution of the problem for the 3D-case is still an open question, which will be in the focus of



**Table 8**  
Optimal measurement configurations for typical spatial manipulators.

Manipulator	Number of measurement configurations	Configurations		
		Configuration #1	Configuration #2	Configuration #3
3-axis SCARA	$m = 2$	$(0^\circ, -90^\circ, L)$ 	$(0^\circ, 90^\circ, 0)$ 	
		$\sum_{k=1}^2 \mathbf{J}^{kT} \mathbf{J}^k = \text{diag} [ 2l_1^2, 2l_2^2, 2, 2, 2 ]$		
4-axis SCARA	$m = 3$	$(0^\circ, 0^\circ, 0, 0^\circ)$ 	$(0^\circ, 120^\circ, 0, 120^\circ)$ 	$(0^\circ, -120^\circ, L, -120^\circ)$ 
		$\sum_{k=1}^3 \mathbf{J}^{kT} \mathbf{J}^k = \text{diag} [ 3l_1^2, 3l_2^2, 3l_3^2, 3, 3, 3, 3 ]$		
2-axis articulated manipulator	$m = 2$	$(0^\circ, 0^\circ)$ 	$(0^\circ, 180^\circ)$ 	
		$\sum_{k=1}^2 \mathbf{J}^{kT} \mathbf{J}^k = \text{diag} [ l_2^2, 2l_2^2, 2, 2 ]$		
3-axis articulated manipulator	$m = 3$	$(0^\circ, 0^\circ, 0^\circ)$ 	$(0^\circ, 120^\circ, 120^\circ)$ 	$(0^\circ, -120^\circ, -120^\circ)$ 
		$\sum_{k=1}^3 \mathbf{J}^{kT} \mathbf{J}^k = \text{diag} [ 0.5(l_2 + l_3)^2, 3l_2^2, 3l_3^2, 3, 3, 3 ]$		

further research. The virtue of these results in the case of 6-axis manipulator is shown in the next section.

## 10. Application example

Now let us apply the obtained results to the calibration of the 6 d.o.f. Kuka KR-270 industrial robot (Fig. 5), which obviously is not a planar manipulator studied in previous sections. However, it is attractive to try the proposed rule of thumb (see Section 9) heuristically, considering this spatial manipulator as set of planar kinematic sub-chains. In particular, it is natural to decompose the manipulator into planar sub-chains composed from the following joints and corresponding links: {joint no. 1}, {joints no.2, 3, 5} and {joints no.4, 6}. Using this decomposition and taking into account the joint limits of industrial robot KR-270, it is possible to generate

four measurement configurations (Table 8) allowing us to identify nine desired parameters: the link length deviations  $\Delta l_1, \dots, \Delta l_3$  and the joint offsets  $\Delta q_1, \dots, \Delta q_6$ . The validity of these configurations for the entire 6-axes manipulator can be easily verified by evaluating the rank of the corresponding calibration Jacobian.

To obtain the desired identification accuracy (0.005 mm for  $\Delta l_i$  and 0.01 deg for  $\Delta q_i$ ), the calibration experiments for each measurement configuration should be repeated several times. Taking into account that conventional measurement systems used in industrial environment (laser trackers) provide the accuracy corresponding to the measurement noise parameter  $\sigma \approx 0.03$  mm, one can get the minimum number of calibration experiments (see Table 3) that in this case is  $m_{\min} = 40$ . It means that the calibration experiments should be repeated 10 times for all configurations presented in Table 8.

**Table 9**

Optimal measurement configurations for calibration of industrial robot KUKA KR-270.

Joint coordinate	Configuration no. 1	Configuration no. 2	Configuration no. 3	Configuration no. 4
$q_1$	$-90^\circ$	$0^\circ$	$90^\circ$	$180^\circ$
$q_2$	$-30^\circ$	$-60^\circ$	$-90^\circ$	$-120^\circ$
$q_3$	$90^\circ$	$-90^\circ$	$-90^\circ$	$90^\circ$
$q_4$	$0^\circ$	$180^\circ$	$90^\circ$	$-90^\circ$
$q_5$	$120^\circ$	$-120^\circ$	$-60^\circ$	$60^\circ$
$q_6$	$-120^\circ$	$120^\circ$	$60^\circ$	$-60^\circ$

To show the efficiency of the proposed heuristic approach, Table 9 presents the identification accuracy for two sets of measurement configurations (calibration plans). The first one, Plan no. 1, corresponds to the regular distribution of the joint coordinates that is usually used in practice [44]. The second one, Plan no. 2, uses the measurement configurations (see Table 8) generated using the proposed rule of thumb. As follows from the obtained results, the proposed technique allowed us to improve the calibration accuracy by a factor of 1.7–4.2. The latter confirms usefulness of this heuristic idea: application of the results obtained for a planar case to spatial manipulators.

In more details, the advantages of the Plan no. 2 are confirmed by the following values. For the linear parameters, the regular plan ensures the identification accuracy 0.010...0.021 mm, while the proposed one allows us to reduce the identification errors to 0.005...0.006 mm. Similarly, for the angular parameters, application of the proposed technique leads to the reduction of the identification errors from 0.019...0.100 mrad to 0.008...0.050 mrad. Those results are also illustrated in Fig. 5, which presents stochastic simulation of the calibration experiments corresponding to two sets of measurement configurations. Corresponding graphs clearly show that the proposed technique provides unbiased estimates of the desired parameters and allows essentially reducing deviations of the identification errors. Hence, summarizing this Section, one may conclude that the developed approach, initially targeted to the planar manipulators, can be also efficiently applied to the spatial manipulators (using some heuristic decomposition of the corresponding kinematic chain).

## 11. Discussion

The main advantage of the results presented in this paper is related to essential *reduction of computational efforts* required for generation of optimal measurement configurations, which are used for geometrical calibration of robotic manipulators. In fact, instead of tedious numerical optimization, simple rules can be applied that yield the set of joint angles satisfying certain trigonometric equations (based on the sums of sines and cosines of the joint coordinates and their combinations, see Table 1). It is proved that, in the planar case, this solution ensures the minimization of the determinant of the covariance matrix (D-criterion), which is often used for the calibration experiments

**Table 10**

Identification accuracy for the regular (no. 1) and proposed (no. 2) plans of calibration experiments.

Parameter	Identification accuracy		Improvement factor
	Plan no. 1	Plan no. 2	
$\Delta l_1$ [mm]	0.015	0.005	3.0
$\Delta l_2$ [mm]	0.021	0.005	4.2
$\Delta l_3$ [mm]	0.010	0.006	1.7
$\Delta q_2$ [mrad]	0.021	0.008	2.6
$\Delta q_3$ [mrad]	0.019	0.009	2.1
$\Delta q_5$ [mrad]	0.100	0.050	2.0

planning. However, in the general case (for spatial manipulators), this statement is not valid anymore, while providing quite good solution completely acceptable in practice. The latter justifies the results utility for wider class of manipulator architectures (Table 10).

Another important question, which is beyond the scope of this paper, is related to the selection of the *optimization criteria* used for the evaluation of the measurement configurations “quality”. Here, the main idea came from the analysis of the information matrix that should be strictly diagonal (which corresponds to the maximum of its determinant). It is clear that other existing optimization criteria [20–27] can be also used, but there is no guarantee that they can produce similar rule of thumb or corresponding solutions are better from engineering view point. Some details concerning comparison of different optimization criteria in calibration experiment planning can be found in our previous work [30].

It should be noted that despite the fact that the original problem was formulated without paying attention to the *joint limits*, the obtained results can be also efficiently applied if the joint limits are wider than  $180^\circ$ . Application of the proposed rule of thumb for this case has been presented in Section 8, where the achieved results are 20–60% better than those obtained with regular and random plans. It is clear that special attention should be paid to the problem where the joint ranges are lower than  $180^\circ$ . In this case some of the optimality conditions (28) cannot be satisfied and a sub-optimal solution should insure minimum of corresponding residuals. However, the difficulty of applying the rule of thumb can only occur when at least two joints have narrow limits and it is required to minimize absolute values of several residuals (28) simultaneously.

**Fig. 6.** Industrial robot Kuka KR-270 TM.

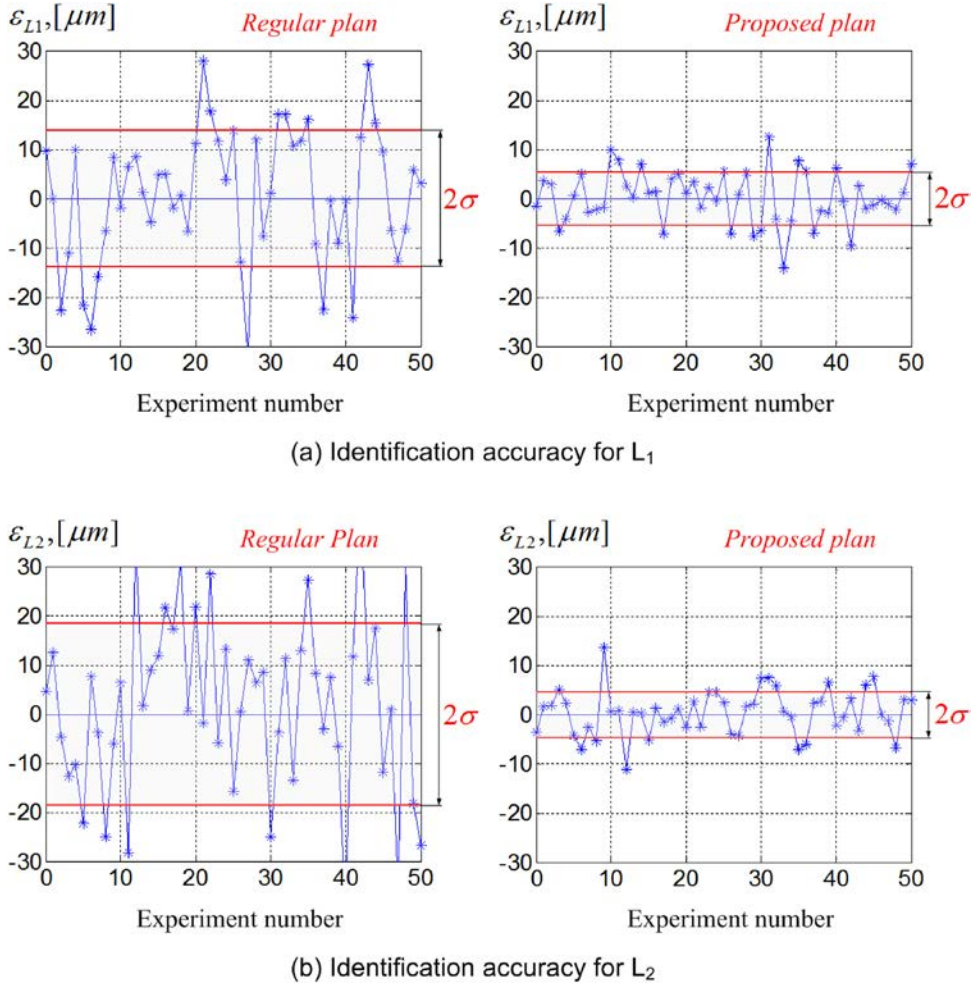


Fig. 7. Comparison of the identification accuracy for two types of calibration plans: (i) regular plan [44]; (ii) proposed plan (measurement noise parameter  $\sigma \approx 0.03$  mm,  $m_{\min} = 40$ ).

Nevertheless, this problem is not common in practice, since such joint ranges usually are typical for the first joint coordinate only. In fact, the joint angle  $q_1$  is not included in the optimality conditions (28), and it can be set arbitrary in the optimal plan developed above.

Besides, the developed rule of thumb can be also used to generate the measurement configurations if there are some *constraints in the Cartesian workspace* (work-cell limits, obstacles, etc.). Since any optimal plan defined by Eq. (28) has a number of redundant variables that can be set arbitrary, it is usually possible to shift the measurement configurations in the joint space to achieve an allowable zone in the Cartesian workspace.

Another question behind the main scope of this paper is related to the *measurement noise impact in actuated joints*. However, as follows from our experience, in practice this factor influence on the identification accuracy is much lower and almost negligible comparing with the measurement errors in Cartesian space. Moreover, it can be strictly proved that this type of errors does not change the optimal measurement configurations since their impact on the parameters identification accuracy (covariance matrix) is described by the constant diagonal term.

Nevertheless, in spite of the fact that obtained results have been efficiently applied to the 3D case and allowed us to improve the identification accuracy, there are several theoretical issues to be studied in future. In particular, special attention should be paid to the optimal pose selection for the calibration of serial kinematic chains with both *revolute* and translation joints mixed in arbitrary order (Figs. 6 and 7).

## 12. Conclusion

The paper presents a new approach for the design of calibration experiments for robotic manipulators that essentially simplifies this procedure and eliminates tedious numerical optimization of measurement poses. The main result is expressed as a system of trigonometric equations describing the set of optimal configurations, which produces strictly diagonal structure of the information matrix. It corresponds to the D-optimality principle known in the design of experiment theory. Relevant technique is formulated in the form of the “rule of thumb” allowing practicing engineer to generate desired measurement configurations in a simple way. The validity of the obtained results and their practical significance were confirmed via simulation studies that deal with two-, three- and four-link planar manipulators. Compared to previous works, the obtained results can be treated as further development of the design-of-experiments theory that is adapted to the specific type of the non-linear models that arise in robot kinematics.

Although the main contributions have been obtained for the planar case, the developed rule has been heuristically generalized for the case of spatial manipulators and successfully applied to several articulated robots. An application example, which deals with the geometric calibration of a Kuka KR-270 industrial robot, also confirms the efficiency of the proposed technique. Nevertheless, a strict theoretical proof of this approach remains the subject of future work that will focus on the optimal pose selection for calibration of non-planar serial and parallel manipulators.



## Acknowledgements

The work presented in this paper was partially funded by the Region "Pays de la Loire", France, by the project ANR COROUSSO, France and FEDER ROBOTEX, France (Grant no. ANR-2010-SEGI-003-02-COROUSSO).

## Appendix A. Appendix A

Analytical solutions for the optimality conditions for 2- and 3-link manipulators

The optimization function for the D-optimality criterion is based on the determinant of the information matrix and for the considered problem can be presented as:

$$\det(\mathbf{C} \times \mathbf{C}^T - \mathbf{S} \times \mathbf{S}^T) \rightarrow \max \quad (38)$$

where the matrices  $\mathbf{C}$ ,  $\mathbf{S}$  are defined by Eq. (23). For illustrative purposes analytical solutions for the cases of 2- and 3-link manipulators are proposed in the following sub-sections.

### A.1. Optimality condition for a 2-link manipulator

For the 2-link manipulator, matrices  $\mathbf{C}$ ,  $\mathbf{S}$  can be written as

$$\mathbf{C} = \begin{bmatrix} m & \sum_{k=1}^m \cos q_2^k \\ \sum_{k=1}^m \cos q_2^k & m \end{bmatrix} \\ \mathbf{S} = \begin{bmatrix} 0 & \sum_{k=1}^m \sin q_2^k \\ \sum_{k=1}^m \sin q_2^k & 0 \end{bmatrix} \quad (39)$$

This allows us to rewrite the optimization problem (38) as

$$\left( m^2 + \left( \sum_{k=1}^m \cos q_2^k \right)^2 - \left( \sum_{k=1}^m \sin q_2^k \right)^2 \right)^2 \\ - \left( 2m \sum_{k=1}^m \cos q_2^k \right)^2 \rightarrow \max \quad (40)$$

that after several transformations leads to

$$\left( m^2 - \left( \left( \sum_{k=1}^m \cos q_2^k \right)^2 + \left( \sum_{k=1}^m \sin q_2^k \right)^2 \right) \right)^2 \rightarrow \max \quad (41)$$

Eq. (41) has an obvious maximum that corresponds to

$$\sum_{k=1}^m \cos q_2^k = 0 \quad \text{and} \quad \sum_{k=1}^m \sin q_2^k = 0 \quad (42)$$

Thus, expression (42) defines optimality condition for calibration plan of 2-link manipulator.

### A.2. Optimality condition for a 3-link manipulator

For the 3-link manipulator, let us introduce following notation

$$x = \sum_{k=1}^m \cos q_2^k; \quad z = \sum_{k=1}^m \cos q_3^k; \quad v = \sum_{k=1}^m \cos (q_2^k + q_3^k) \\ y = \sum_{k=1}^m \sin q_2^k; \quad u = \sum_{k=1}^m \sin q_3^k; \quad w = \sum_{k=1}^m \sin (q_2^k + q_3^k) \quad (43)$$

Then, the matrices  $\mathbf{C}$ ,  $\mathbf{S}$  can be written as

$$\mathbf{C} = \begin{bmatrix} m & x & v \\ x & m & z \\ v & z & m \end{bmatrix}; \quad \mathbf{S} = \begin{bmatrix} 0 & y & w \\ y & 0 & u \\ w & u & 0 \end{bmatrix} \quad (44)$$

This allows us to rewrite the optimization problem (38) as

$$\left( m^3 + 2yzw + 2xzv - 2yuv + 2xuz - m(x^2 + y^2 + z^2 + u^2 + v^2 + w^2) \right)^2 \\ \rightarrow \max \quad (45)$$

for which it is required to find a maximum with respect to the angle coordinates  $q_2^k, q_3^k, q_{23}^k, k = \overline{1, m}$ . Expression (45) depends on the sum of cosines and sines of these arguments. For the convenience purposes these sums are substituted by single unknown parameters.

Using the above defined assumptions, solution of the optimization problem is reduced to finding the extremum of the inner function and to extracting solutions that correspond to the maximum. In order to find the extremum let us compute partial derivatives of expression (45) with respect to all unknown parameters. As a result, one can obtain the following system of equations

$$m \times x = z \times v + u \times w \quad m \times y = z \times w - u \times v \\ m \times z = x \times v + y \times w \quad m \times u = x \times w - y \times v \\ m \times v = x \times z - y \times u \quad m \times w = y \times z + x \times u \quad (46)$$

that should be solved with respect to  $x, y, z, u, v, w$ . This system of equations has the following solutions

$$\left\{ \begin{array}{l} v = 0 \\ w = 0 \\ z = 0 \\ u = 0 \\ x = 0 \\ y = 0 \end{array} \right\} \cup \left\{ \begin{array}{l} v^2 + w^2 = m^2 \\ u = 0 \\ z = \mu \times m \\ x = \mu \times v \\ y = \mu \times w \end{array} \right\} \\ \cup \left\{ \begin{array}{l} z^2 + u^2 = m^2 \\ w = 0 \\ v = \mu \times m \\ x = \mu \times z \\ y = \mu \times u \end{array} \right\} \cup \left\{ \begin{array}{l} u = 0 \\ v = 0 \\ z = \mu_1 \times m \\ w = \mu_2 \times m \\ x = 0 \\ y = \mu_1 \mu_2 m \end{array} \right\} \quad (47)$$

where  $\mu = \pm 1, \mu_1 = \pm 1, \mu_2 = \pm 1$ .

Substituting the first solution of (47) in (45) one can obtain that  $m^3$  is the maximum. The second and the third systems of (47) have two solutions that bring to zero expression (45). It is clear that such solutions do not ensure the maximum of the squared function. Similarly, the fourth solution does not bring maximize expression (45).

As a result, a necessary and sufficient condition to maximize (45) is

$$\sum_{k=1}^m \cos q_2^k = 0; \quad \sum_{k=1}^m \cos q_3^k = 0 \quad \sum_{k=1}^m \cos (q_2^k + q_3^k) = 0 \\ \sum_{k=1}^m \sin q_2^k = 0; \quad \sum_{k=1}^m \sin q_3^k = 0; \quad \sum_{k=1}^m \sin (q_2^k + q_3^k) = 0 \quad (48)$$

That can be interpreted on the plane as a zero sum of unit vectors based on the optimal angles.

## References

- [1] Roth ZS, Mooring B, Ravani B. An overview of robot calibration. *IEEE J Rob Autom* 1987;3:377–85.

- [2] Elatta A, Gen LP, Zhi FL, Daoyuan Y, Fei L. An overview of robot calibration. *Inform Technol J* 2004;3:74–8.
- [3] Mooring BW, Roth ZS, Driels MR. *Fundamentals of manipulator calibration*. New York, NY: Wiley; 1991.
- [4] Pashkevich A. Computer-aided generation of complete irreducible models for robotic manipulators. In: *The third international conference of modelling and simulation*. 2001. p. 293–8.
- [5] Nubiola A, Bonev IA. Absolute robot calibration with a single telescoping ball-bar. *Precis Eng* 2014;38:472–80.
- [6] Santolaria J, Brosted F-J, Velázquez J, Jiménez R. Self-alignment of on-board measurement sensors for robot kinematic calibration. *Precis Eng* 2013;37:699–710.
- [7] Hollerbach JM. *A survey of kinematic calibration*. The robotics review 1. Cambridge, MA, USA: MIT Press; 1989. p. 207–42.
- [8] Hayati SA. Robot arm geometric link parameter estimation. In: *Decision and control, 1983, The 22nd IEEE conference on*: IEEE. 1983. p. 1477–83.
- [9] Stone HW. *Kinematic modeling, identification, and control of robotic manipulators*. MA, USA: Springer; 1987.
- [10] Zhuang H, Roth ZS, Hamano F. A complete and parametrically continuous kinematic model for robot manipulators. *IEEE J Rob Autom* 1992;8:451–63.
- [11] Chen Y, Gao J, Deng H, Zheng D, Chen X, Kelly R. Spatial statistical analysis and compensation of machining errors for complex surfaces. *Precis Eng* 2013;37:203–12.
- [12] Klimchik A, Pashkevich A, Chablat D, Hovland G. Compliance error compensation technique for parallel robots composed of non-perfect serial chains. *Rob Comput Integr Manuf* 2013;29:385–93.
- [13] Shi H, Su H-J, Dagalakis N, Kramar JA. Kinematic modeling and calibration of a flexure based hexapod nanopositioner. *Precis Eng* 2013;37:117–28.
- [14] Ikits M, Hollerbach JM. Kinematic calibration using a plane constraint. In: *Robotics and automation, 1997 proceedings, 1997 IEEE international conference on*: IEEE. 1997. p. 3191–6.
- [15] Mirman CR, Gupta KC. Compensation of Robot joint variables using special Jacobian matrices. *J Rob Syst* 1992;9:113–37.
- [16] Slamani M, Nubiola A, Bonev IA. Modeling and assessment of the backlash error of an industrial robot. *Robotica* 2012;30:1167–75.
- [17] Sun Y, Hollerbach JM. Observability index selection for robot calibration. In: *Robotics and automation, 2008 ICRA, 2008 IEEE international conference on*. 2008. p. 831–6.
- [18] Sun Y, Hollerbach JM. Active robot calibration algorithm. In: *Robotics and automation, 2008 ICRA, 2008 IEEE international conference on*: IEEE. 2008. p. 1276–81.
- [19] Hollerbach J, Khalil W, Gautier M. Model identification. In: Siciliano B, Khatib O, editors. *Springer handbook of robotics*. Berlin Heidelberg: Springer; 2008. p. 321–44.
- [20] Zhuang H, Wu J, Huang W. Optimal planning of robot calibration experiments by genetic algorithms. In: *Robotics and automation 1996. Proceedings, 1996. IEEE international conference on*: IEEE. 1996. p. 981–6.
- [21] Daney D, Papegay Y, Madeline B. Choosing measurement poses for robot calibration with the local convergence method and Tabu search. *Int J Rob Res* 2005;24:501–18.
- [22] Atkinson AC, Donev AN. *Optimum experimental designs*. Oxford statistical science series, vol. 8. Oxford, UK: Oxford University Press; 1992.
- [23] Borm J-H, Menq C-H. Determination of optimal measurement configurations for robot calibration based on observability measure. *Int J Rob Res* 1991;10:51–63.
- [24] Khalil W, Gautier M, Enguehard C. Identifiable parameters and optimum configurations for robots calibration. *Robotica* 1991;9:63–70.
- [25] Daney D. Optimal measurement configurations for Gough platform calibration. In: *Robotics and automation, 2002 proceedings ICRA'02, IEEE international conference on*: IEEE. 2002. p. 147–52.
- [26] Nahvi A, Hollerbach JM. The noise amplification index for optimal pose selection in robot calibration. In: *Robotics and automation, 1996 proceedings, 1996 IEEE international conference on*: IEEE. 1996. p. 647–54.
- [27] Klimchik A, Wu Y, Caro S, Pashkevich A. Design of experiments for calibration of planar anthropomorphic manipulators. In: *Advanced intelligent mechatronics (AIM), 2011 IEEE/ASME international conference on*: IEEE. 2011. p. 576–81.
- [28] Zhuang H, Wang K, Roth ZS. Optimal selection of measurement configurations for robot calibration using simulated annealing. In: *Robotics and automation, 1994 proceedings, 1994 IEEE international conference on*: IEEE. 1994. p. 393–8.
- [29] Imoto J, Takeda Y, Saito H, Ichiryu K. Optimal kinematic calibration of robots based on maximum positioning-error estimation (theory and application to a parallel-mechanism pipe bender). In: *Computational Kinematics*. Berlin, Heidelberg: Springer; 2009. p. 133–40.
- [30] Klimchik A, Wu Y, Pashkevich A, Caro S, Furet B. Optimal selection of measurement configurations for stiffness model calibration of anthropomorphic manipulators. *Appl Mech Mater* 2012;162:161–70.
- [31] Bernhardt R, Albright S. *Robot calibration*. United Kingdom: Chapman and Hall; 1993.
- [32] Le QV, Ng AY. Joint calibration of multiple sensors. In: *Intelligent robots and systems, 2009 IROS, 2009 IEEE/RSJ international conference on*: IEEE. 2009. p. 3651–8.
- [33] Beyer L, Wulfsberg J. Practical robot calibration with ROSY. *Robotica* 2004;22:505–12.
- [34] Liu Y, Jiang Z, Liu H, Xu W. Geometric parameter identification of a 6-DOF space robot using a laser-ranger. *J Rob* 2012;2012:11, <http://dx.doi.org/10.1155/2012/587407>. Article ID 587407.
- [35] Park I, Lee B, Cho S, Hong Y, Kim J. Laser-based kinematic calibration of robot manipulator using differential kinematics. *IEEE/ASME Trans Mechatron* 2012;17:1059–67.
- [36] Liu J, Zhang Y, Li Z. Improving the positioning accuracy of a neurosurgical robot system. *IEEE/ASME Trans Mechatron* 2007;12:527–33.
- [37] Santolaria J, Aguilar J-J, Yagüe J-A, Pastor J. Kinematic parameter estimation technique for calibration and repeatability improvement of articulated arm coordinate measuring machines. *Precis Eng* 2008;32:251–68.
- [38] Lightcap C, Hamner S, Schmitz T, Banks S. Improved positioning accuracy of the PA10-6CE robot with geometric and flexibility calibration. *IEEE Trans Rob* 2008;24:452–6.
- [39] Santolaria J, Conte J, Ginés M. Laser tracker-based kinematic parameter calibration of industrial robots by improved CPA method and active retroreflector. *Int J Adv Manuf Technol* 2013:1–20.
- [40] Williams I, Hovland G, Brogardh T. Kinematic error calibration of the gantry-tau parallel manipulator. In: *Robotics and automation, 2006 ICRA, 2006 proceedings, 2006 IEEE international conference on*: IEEE. 2006. p. 4199–204.
- [41] Gantmakher FR. *The theory of matrices*. 1. New York, USA: Chelsea Publishing Company; 1959.
- [42] Joubair A, Bonev IA. Comparison of the efficiency of five observability indices for robot calibration. *Mech Mach Theory* 2013;70:254–65.
- [43] Klimchik A, Pashkevich A, Wu Y, Caro S, Furet B. Design of calibration experiments for identification of manipulator elastostatic parameters. *Appl Mech Mater* 2012;162:161–70.
- [44] Dumas C, Caro S, Garnier S, Furet B. Joint stiffness identification of six-revolute industrial serial robots. *Rob Comput Integr Manuf* 2011;27:881–8.